J. Electrochem. Sci. Eng. **14(5)** (2024) 617-629; http://dx.doi.org/10.5599/jese.2350

Open Access : : ISSN 1847-9286
www.jESE-online.org

Original scientific paper

Design of high-performance electrochemical sensor based on SnS_2 nanoplates and ionic liquid-modified carbon paste electrode for determination of hydrazine in water samples

Afsaneh Haji Alizadeh[1,✉], Abdulhamid Morshidi Nozar[2] and Samaneh Salemi Najaf Abadi[3]

[1]*Department of Chemistry, Sirjan Branch, Islamic Azad University, Sirjan, Iran*
[2]*Department of Chemical Engineering, Sirjan Branch, Islamic Azad University, Sirjan, Iran*
[3]*Department of Basic Science, Sirjan Branch, Islamic Azad University, Sirjan, Iran*

Corresponding authors: ✉ a.hajializadeh@yahoo.com

Received: April 18, 2024; Accepted: August 26, 2024; Published: September 30, 2024

Abstract

Designing effective and accurate analytical techniques to determine hydrazine is essential for preserving the environment. Herein, an electrochemical sensor based on a carbon paste electrode (CPE) modified with SnS_2 nanoplates (SnS_2NPs) and ionic liquid (IL) was presented for determination of hydrazine in water samples. The SnS_2NPs were synthesized using the hydrothermal method and characterized through field emission scanning electron microscope, Fourier transform infrared spectrometer and energy dispersive spectroscopy. The use of cyclic voltammetry in electrochemical investigations has shown that incorporating IL and SnS_2NPs in an electrochemical sensor significantly improves its efficiency. These results in a considerable increase in the oxidation peak current and a decrease in the oxidation peak potential of hydrazine compared to an unmodified CPE. The method of differential pulse voltammetry was utilized to accurately measure the quantity of hydrazine. The SnS_2NPs/ILCPE showed improved sensing capabilities, resulting in a noticeable sensitivity of 0.0747 µA/µM and a low limit of detection of 0.05 µM for a broad linear range of hydrazine concentration from 0.08 µM to 450.0 µM. In addition, the SnS2NPs/ILCPE sensor was successfully utilized to measure the amount of hydrazine present in water samples, with a recovery range of 96.0 to 104.4 %. The relative standard deviation was found to be lower than 3.6 % (n = 5), indicating that the developed sensor is suitable for accurately determining hydrazine in water samples with high sensitivity.

Keywords

Electrochemical sensing, hydrazine, tin disulfide nanoplates, ionic liquid, real water samples

Introduction

According to the World Health Organization (WHO) and the United States Environmental Protection Agency (USEPA), hydrazine (N_2H_4) and its derivatives are recognized as strong carcinogens, with a maximum allowable concentration of 0.1 ppm. Hydrazine is a crucial chemical that acts as a potent reducing agent. These harmful chemicals are frequently present in aerospace, military, agriculture, pharmaceutical, and industrial environments, especially in industrial and agricultural sewage [1-5]. It is important to note that hydrazine is highly mutagenic and carcinogenic, causing severe problems in the liver and brain. It can also damage deoxyribonucleic acid (DNA) and affect the nervous system [5-7]. In addition to its high solubility, there is significant concern regarding hydrazine contamination of soil and water [8]. Considering the environmental concerns, it is important to develop simple, fast, and low-cost methods for the determination of hydrazine in water samples to aid in environmental monitoring and control. Therefore, it is necessary to develop an effective extraction method before a powerful analytical performance for the preconcentration and determination of pollutants by gas chromatography-mass spectrometry, fluorescence spectroscopy, flow injection analysis, high-performance liquid chromatography, and colorimetry [8-13]. Some methods offer high accuracy, sensitivity, and selectivity. However, their usage can be challenging due to time-consuming measurement processes, high-cost instruments, and a need for highly skilled technicians.

An electrochemical approach is reliable for detecting hydrazine with enough precision and sensitivity. To meet this need, the creation of a top-performing hydrazine sensor is a priority. This has spurred efforts to produce a crucial electrochemical sensor capable of effectively and simultaneously identifying hydrazine. The simplicity, affordability, real-time capability, efficiency, and sensitivity of electrochemical detection make it the preferred method for analyzing compounds within a broad range of operations [14-23]. This is because they limit their extensive applications. Solid carbon-based electrodes are widely used in electroanalysis due to their low background current, broad potential window, low cost, rich surface chemistry, chemical inertness and suitability for various sensing and detection applications [23-25].

Carbon paste electrodes (CPEs) are prepared by mixing graphite powder and pasting liquid such as paraffin oil. The advantages of CPEs have recently drawn the attention of researchers, who have exploited these advantages for a variety of measurements, especially voltammetry, as evidenced by numerous studies [26-29]. The modification of electrodes through the development and application of functional materials is crucial to enhance their electrochemical performance. These materials should provide high electrical conductivity, high surface area, and compatibility [30-32].

Nanostructured materials have outstanding potential for use as base materials in emerging technologies. Nanomaterials have become increasingly popular in recent years for use in electrochemical sensing applications. This is due to their excellent catalytic activity, high adsorption capacity, high surface-to-volume ratio, and high electrical conductivity compared to their bulk counterparts [34-37]. Various types of electrode modifiers have been employed to develop high-performance electrochemical sensors. These modifiers include carbon nanomaterials like fullerene, graphene, and carbon nanotubes, metal and metal oxide nanoparticles, metal chalcogenides, metal-organic frameworks, and many others. Among these, layered metal dichalcogenides are a relatively new class of 2D materials with unique thickness-dependent band gaps and exceptional electrochemical and thermal properties. As a result, they have been widely used in various applications [38-40]. Tin disulfide (SnS_2) is a type of layered metal dichalcogenide. It is a well-known n-type semiconductor with an indirect bandgap of 2.43 eV [41]. Due to its non-toxic, chemically stable, and excellent physical and

chemical properties [42], SnS_2 has been widely utilized in the manufacturing of batteries [43], supercapacitors [44], gas sensors [45], photocatalysts [46], and electrochemical sensors [47-49]. An ionic liquid (ILs) has become a popular choice for volumetric analysis design due to its unique features, including possible catalytic activity, electrochemical stability, low toxicity, and excellent conductivity [50,51]. In CPE preparation, IL can fully replace pasting liquid and act as a binder. IL can be used as an additional component of CPE. It has been reported that an IL-based CPE performs better than conventional CPEs, which contain non-conductive binders, such as paraffin oil.

The objective of this study was to determine hydrazine levels using an SnS_2NPs/IL-modified CPE sensing platform with electrochemical performance and to test it for the analysis of hydrazine in some water samples.

Experimental

Instrumentation

In this work, the AUTOLAB PGSTAT 302N potentiostat/galvanostat was used for electrochemical investigations. A reference electrode of Ag/AgCl/3.0 M KCl was utilized. Pt wire and SnS_2 nanoparticles were used as the counter and working electrodes, respectively, in an electrochemical cell. Electrochemical data were processed using GPES software.

Reagents

Graphite powder, paraffin oil, IL (n-hexyl-3-methylimidazolium hexafluoro phosphate), sodium hydroxide, and phosphoric acid were obtained from Sigma-Aldrich. Merck company provided tin (II) chloride dihydrate ($SnCl_2{\cdot}2H_2O$), thiourea and other reagents for the synthesis of SnS_2NPs.

Synthesis of SnS_2 NPs

SnS_2 nanoparticles were synthesized using a straightforward hydrothermal method. 2 mmol of $SnCl_2{\cdot}2H_2O$ (0.45 g) and 12 mmol of $SC(NH_2)_2$ (0.91 g) were dissolved in 80 mL of deionized water under magnetic stirring for 15 minutes. After being prepared, the solution was placed in a Teflon-lined stainless steel autoclave and subjected to hydrothermal treatment at 190ºC for 12 hours. After being allowed to cool naturally to ambient temperature, the resulting precipitate was collected using centrifugation, washed multiple times with ethanol and deionized water, and then dried under vacuum at 70 °C for 15 hours.

Preparation of modified CPE

The SnS_2NPs/ILCPE was prepared by mixing graphite powder and SnS_2NPs in the ratio of 95:5 (w/w) and paraffin oil and IL in the ratio of 8:2 (v/v). The mixture was then homogenized in an agate mortar using a pestle. The obtained paste was packed in a glass tube, and a copper wire was used for electrical contact.

Results and discussion

Characterization of SnS_2NPs

The FTIR spectrum of SnS_2 nanoparticles was collected in the range of 400 to 4000 cm^{-1} and presented in Figure 1. The absorption peak at 622 cm^{-1} corresponds to the Sn-S stretching vibration. Stretching vibration and bending vibration of -OH groups from free or adsorbed solvent molecules can be observed at around 1630 and 3437 cm^{-1}, respectively.

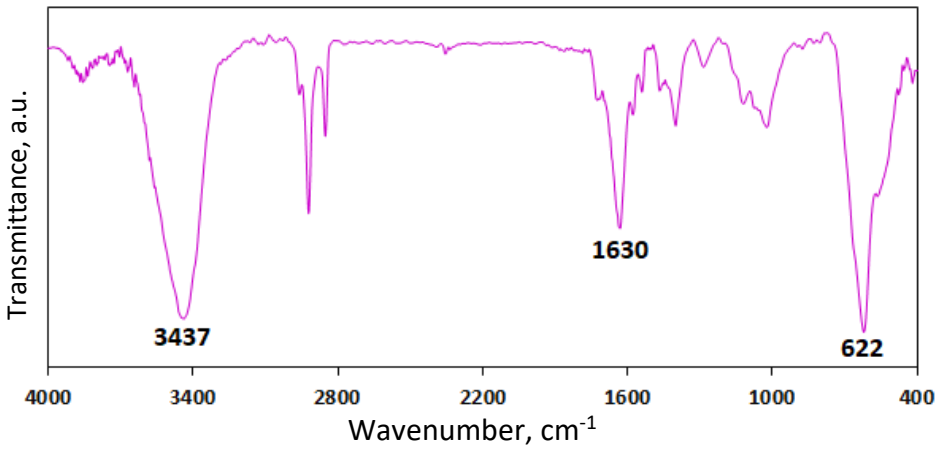

Figure 1. *FT-IR spectrum of SnS_2 NPs*

The morphology and structure of the SnS_2 nanoparticles that were prepared were studied using FE-SEM (as shown in Figure 2). The SnS_2 displayed a layered structure that was two-dimensional (2D). Additionally, the SnS_2 nanoparticles were stacked on top of each other, creating a flower-like morphology. Figure 3 revealed Sn and S as the main elements in the structure of SnS_2.

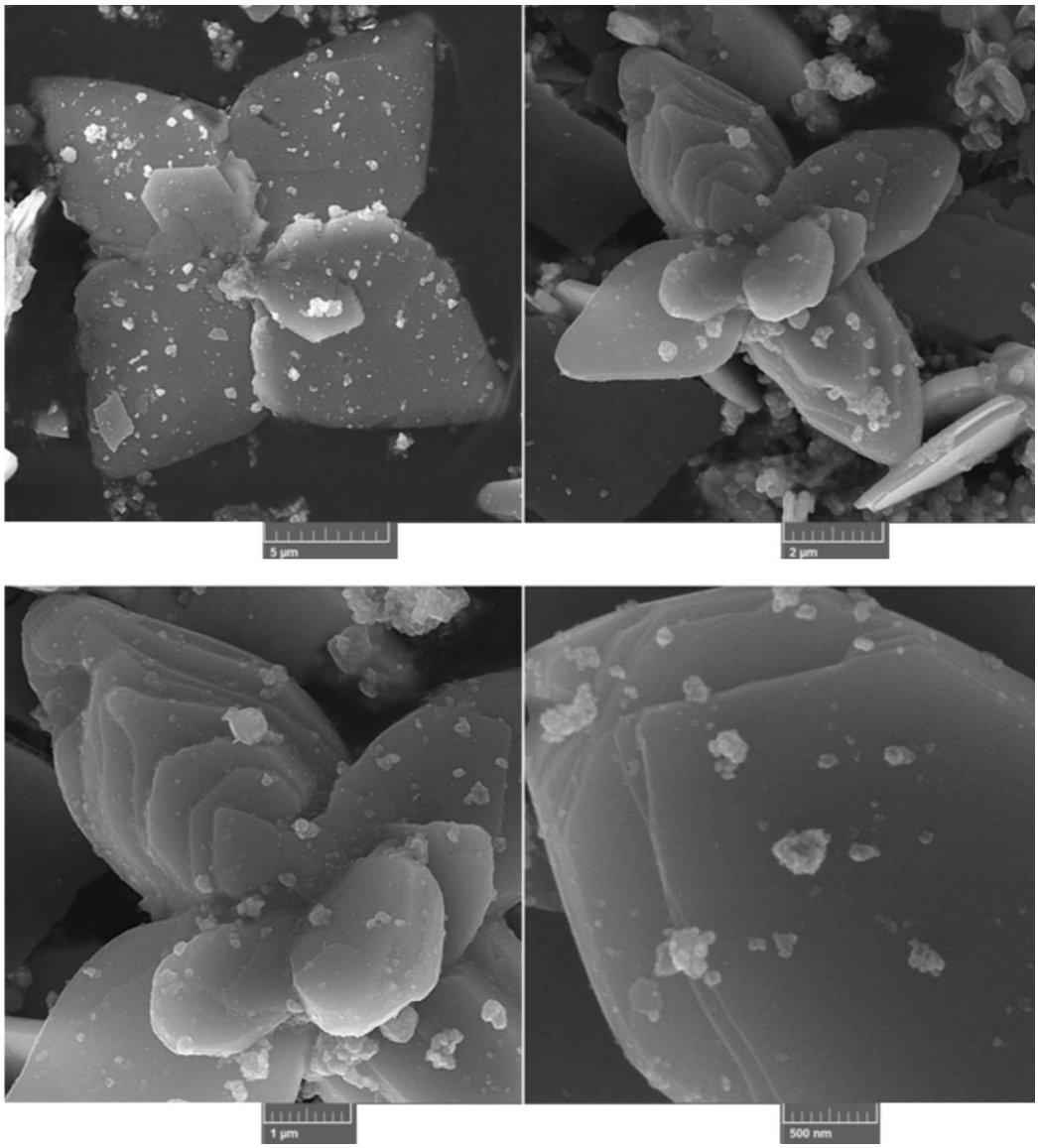

Figure 2. *FE-SEM images of SnS_2NPs at different magnifications*

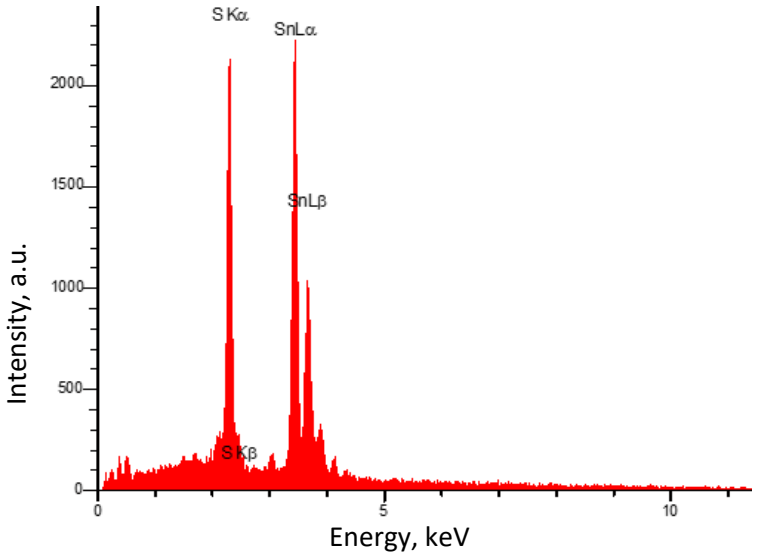

Figure 3. *EDS spectrum of SnS_2NPs*

Electrochemical behavior of hydrazine at the surface of various electrodes

Recorded voltammograms of hydrazine were investigated at SnS_2NPs/ILCPE under different pH values (4-9) of 0.1 M phosphate buffer solution (PBS) to study pH effects. Based on the results obtained, it was found that the oxidation potential decreased with an increase in pH. This suggests that protons play a crucial role in the oxidation mechanism process of hydrazine. Moreover, the electrochemical studies and measurements showed that the highest peak current was observed at pH 7.0, which is considered the optimum pH in all experiments.

In the next step, the response of hydrazine was recorded on the surface of unmodified CPE (Figure 4, curve a), and SnS_2NPs/ILCPE (Figure 4, curve b). At the SnS_2NPs/ILCPE surface, the oxidation potential of hydrazine was reduced compared to unmodified CPE. In addition, the modification of CPE resulted in an enhancement of the oxidation current of hydrazine. These observations can be related to the improvement in surface area along with the enhancement of the electrical conductivity of the modified CPE due to the presence of SnS_2NPs and IL.

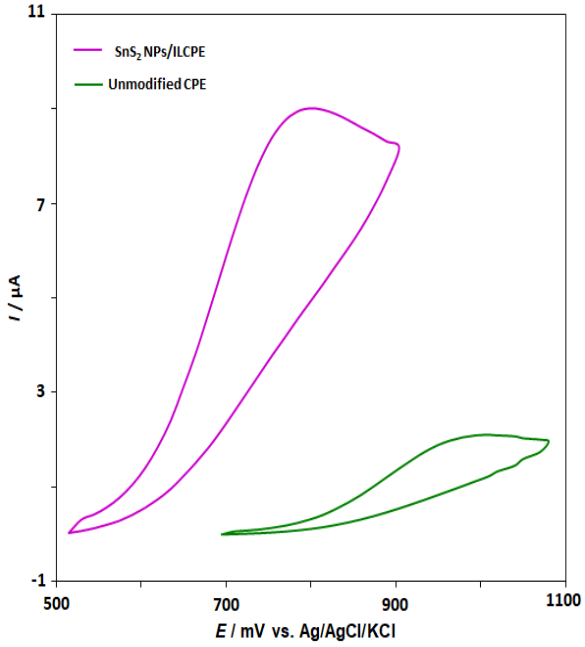

Figure 4. *Cyclic voltammograms at 50 mV s^{-1} of 100.0 µM hydrazine recorded at the surface of: (-) unmodified CPE and (-) SnS_2NPs/ILCPE*

Effect of potential scan rate

The voltammograms of hydrazine were recorded on the surface of SnS_2NPs/ILCPE, with a scan rate range of 10 to 400 mV s^{-1}, Figure 5. The regression linear equation $I_{pa} = 1.0693v^{1/2} - 0.3468$ was obtained (Figure 6), indicating that the oxidation reaction of hydrazine is a diffusion-controlled process.

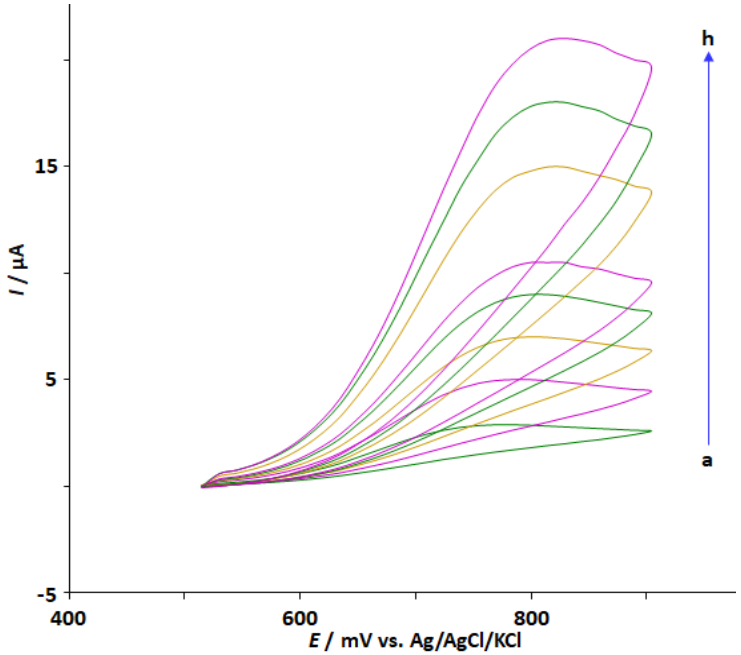

Figure 5. *Cyclic voltammograms of 75.0 µM hydrazine on SnS_2NPs/ILCPE at different scan rates: (a) 10, (b) 25, (c) 50, (d) 75, (e) 100, (f) 200, (g) 300, and (h) 400 mV s^{-1}*

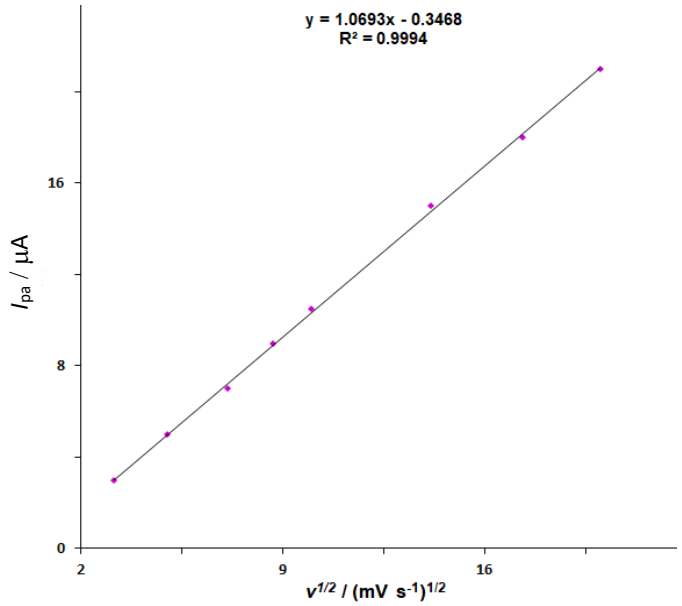

Figure 6. *The relationship between I_{pa} and $v^{1/2}$ for electro-oxidation of 75.0 µM hydrazine on SnS_2NPs/ILCPE*

Chronoamperometric studies

During the hydrazine oxidation process on the surface of SnS_2NPs/ILCPE, the chronoamperometric method with an applied potential of 850 mV was used to determine the diffusion coefficient (*D*) of hydrazine (Figure 7). Figure 8 illustrates the Cottrell plots relative to hydrazine oxidation on the surface of modified CPE. Then, a linear dependence was observed for the slopes of Cottrell plots when plotted against the corresponding concentrations of hydrazine (Figure 9). Using the obtained slope and based on the Cottrell equation, the value of *D* was calculated to be about 3.9×10^{-6} cm^2 s^{-1}.

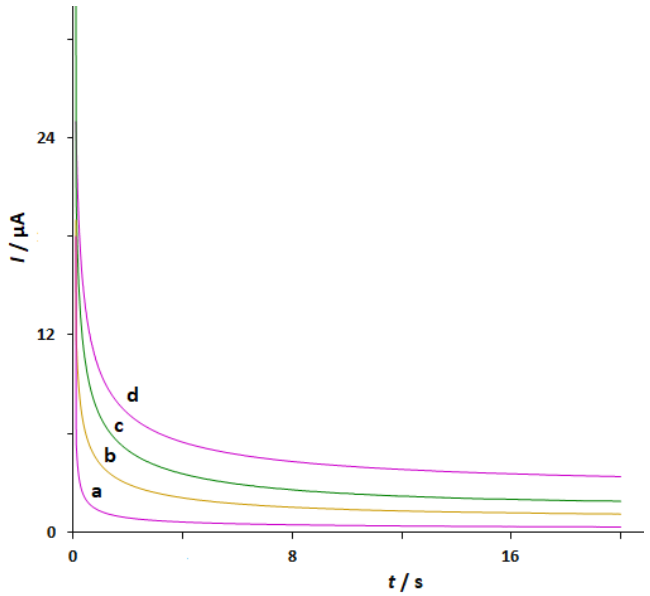

Figure 7. *Chronoamperograms of: (a) 0.1, (b) 0.2, (c) 0.33 and (d) 0.43 mM hydrazine recorded at SnS_2NPs/ILCPE*

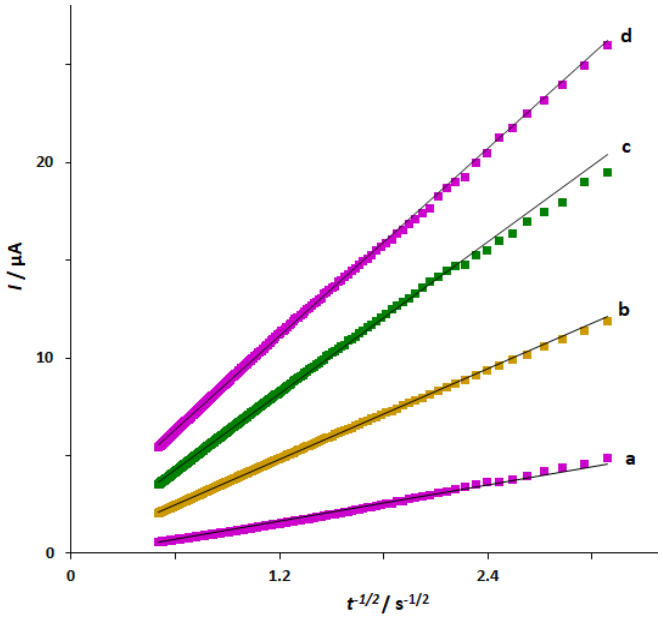

Figure 8. *Cottrell plots obtained from chronoamperograms in Fig. 7*

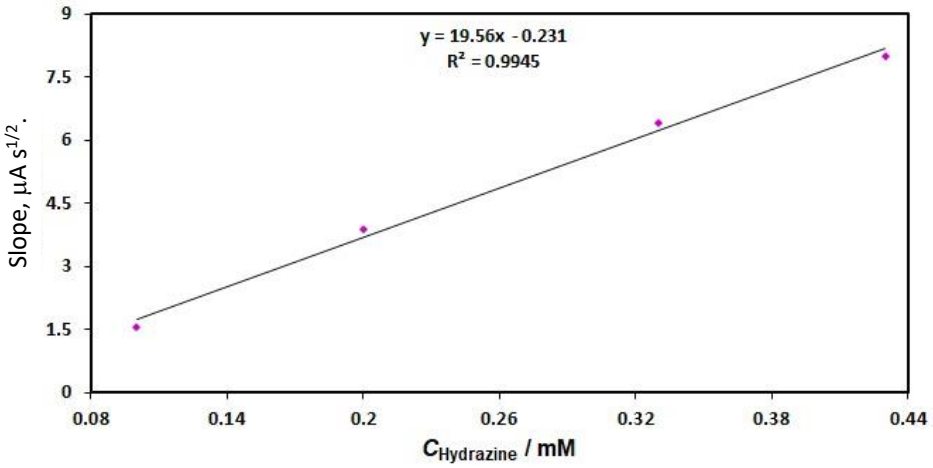

Figure 9. *Slopes of Cottrell plots in Figure 8 against hydrazine concentration*

Differential pulse voltammetry (DPV) measurements

Differential pulse voltammograms (DPVs) of hydrazine on the surface of SnS_2NPs/ILCPE are shown in Figure 10. DPV measurements were performed for different hydrazine concentrations using optimized parameters (step potential (0.01 V) and pulse amplitude (0.025 V)). It is observed that there was a linear relationship between current and hydrazine concentration in the range of 0.08-450.0 µM, with the regression linear equation: I_{pa} = 0.0747 $C_{Hydrazine}$ + 1.0918 (R^2 = 0.9995) (as shown in Figure 11). The limit of detection (LoD) was calculated based on Equation (1):

$$LoD = 3S/m \quad (1)$$

where m is the slope value obtained from the calibration plot and S is the standard deviation (9 measurements of blank solution). The LoD was found to be 0.05 µM.

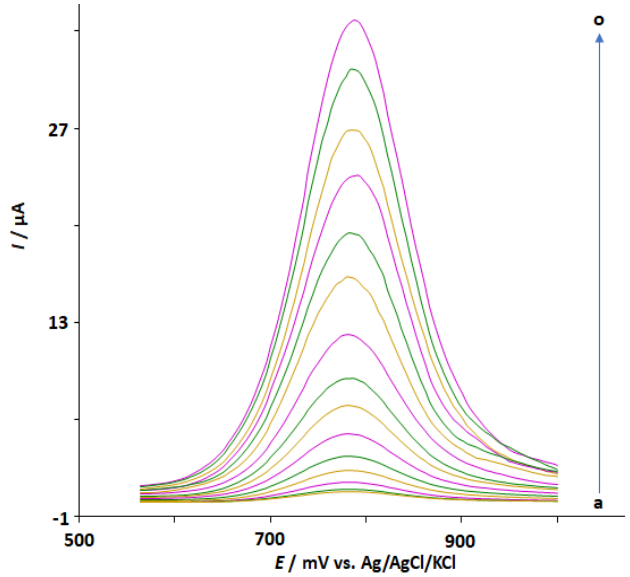

Figure 10. *DPVs of hydrazine at concentrations of (a) 0.08; (b) 2.5; (c) 7.5; (d) 15.0; (e) 30.0; (f) 50.0; (g) 75.0; (h) 100.0; (i) 150.0; (j) 200.0; (k) 250.0; (l) 300.0; (m) 350.0; (n) 400.0 and (o) 450.0 µM*

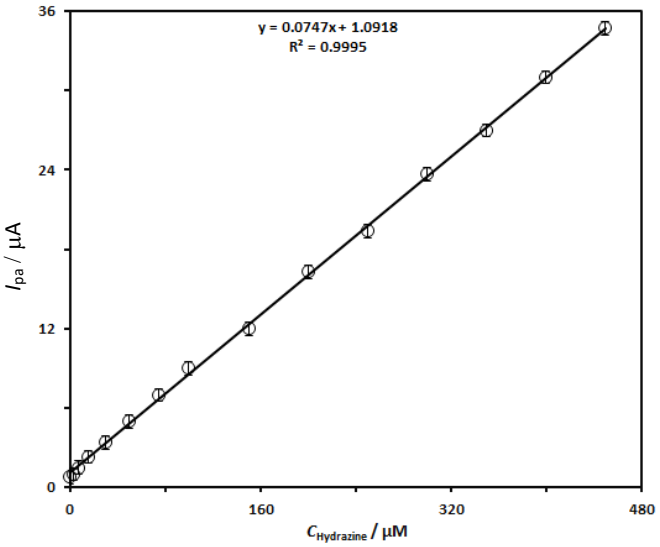

Figure 11. *Plot of I_{pa} as a function of hydrazine concentration*

Table 1 shows the analytical performance of the designed sensor in this work in comparison to earlier hydrazine sensors already reported in the literature.

Table 1. *Analytical performances of different electrode-based assays for hydrazine detection*

Modified electrode	Linear range	LoD, µM	Ref.
SnS_2NPs/ILCPE	0.08 to 450.0 µM	0.05 µM	This work
NiCo-layered double hydroxides@hierarchical Ni nanowires/glassy carbon electrode	10 µM to 8 mM	0.29	[15]
Ag-Ni/reduced graphene oxide/glassy carbon electrode	1.0 µM to 1.05 mM	0.3	[17]
CuO nanosheets decorated the surface of cellulose acetate butyrate/glassy carbon electrode	0.5 to 100 mM	0.15	[52]
Ag@Fe_3O_4 core-shell nanospheres/glassy carbon electrode	0.25 µM to 3.4 mM	0.06	[53]

Real sample analysis

The SnS_2NPs/ILCPE's ability to detect hydrazine in water samples was tested using a standard addition strategy, as shown in Table 2. The recovery values in the range of 96.0 to 104.4 % demonstrate the developed sensor's strong ability to accurately determine hydrazine in real samples.

Table 2. *Analysis of hydrazine in real water samples using SnS_2NPs/ILCPE*

Sample	Concentration, µM		Recovery, %	RSD, %
	Added	Founded		
River water	5.0	4.9	98.0	3.6
	7.0	7.1	101.4	1.9
	9.0	9.4	104.4	2.5
	11.0	10.9	99.1	2.2
Tap water	5.0	5.1	102.0	2.3
	7.5	7.2	96.0	3.5
	10.0	10.4	104.0	1.8
	12.5	12.4	99.2	2.7

Conclusion

In this study, we successfully synthesized and characterized SnS_2NPs. An efficient electrochemical hydrazine sensor was developed by modifying CPE with SnS_2NPs and IL. Studies conducted on the performance of the modified electrode (SnS_2NPs/ILCPE) have yielded positive results by enhancing peak current and minimizing peak potential for the oxidation of hydrazine. Additionally, the modified CPE has displayed a strong response in determining hydrazine levels. Linear dependence between peak current intensity and hydrazine concentration from 0.08 to 450.0 µM was observed with a high sensitivity of 0.0747 µA/µM and a LoD of 0.05 µM in the SnS_2NPs/ILCPE sensor under optimal conditions. The SnS_2NPs/ILCPE sensor developed in this study was successfully applied for real sample analysis, with satisfactory recovery results (96.0-104.4 %) and low RSD values (≤3.6 %).

References

[1] N. S. K. Gowthaman, S. Shankar, S. Abraham John, Ultrasensitive and selective hydrazine determination in water samples using Ag-Cu heterostructures grown indium tin oxide electrode by environmentally benign method, *ACS Sustainable Chemistry & Engineering* **6(12)** (2018) 17302-17313. https://doi.org/10.1021/acssuschemeng.8b04777

[2] N. M. A. K. Jailani, M. Chinnasamy, N. S. K. Gowthaman, Facile one-pot synthesis of CuO nanospheres: Sensitive electrochemical determination of hydrazine in water effluents, *Journal of Electrochemical Science and Engineering* **12(3)** (2022) 439-449. https://doi.org/10.5599/jese.1207

[3] C. Wang, L. Zhang, Z. Guo, J. Xu, H. Wang, K. Zhai, X. Zhuo, A novel hydrazine electrochemical sensor based on the high specific surface area graphene, *Microchimica Acta* **169** (2010) 1-6. https://doi.org/10.1007/s00604-010-0304-6

[4] J. Deng, S. Deng, Y. Liu, Highly sensitive electrochemical sensing platform for hydrazine detection, *International Journal Electrochemical Science* **13** (2018) 3566-3574. https://doi.org/10.20964/2018.04.38

[5] S. Garrod, M. E. Bollard, A. W. Nicholls, S. C. Connor, J. Connelly, J. K. Nicholson, E. Holmes, Integrated metabonomic analysis of the multiorgan effects of hydrazine toxicity in the rat, *Chemical Research in Toxicology* **18** (2005) 115-122. https://doi.org/10.1021/tx0498915

[6] L. Cui, Z. Peng, C. Ji, J. Huang, D. Huang, J. Ma, S. Zhang, X. Qian, Y. Xu, Hydrazine detection in the gas state and aqueous solution based on the Gabriel mechanism and its imaging in living cells, *Chemical Communications* **50 (12)** (2014) 1485-1487. https://doi.org/10.1039/C3CC48304E

[7] S. Dutta, C. Ray, S. Mallick, S. Sarkar, A. Roy, T. Pal, Au@ Pd core–shell nanoparticles-decorated reduced graphene oxide: a highly sensitive and selective platform for electrochemical detection of hydrazine, *RSC Advances* **5 (64)** (2015) 51690-51700. https://doi.org/10.1039/C5RA04817F

[8] P. B. Deroco, I. G. Melo, L. S. R. Silva, K. I. B. Eguliuz, G. L. Salazar-Banda, O. Fatibello-Filho, Carbon black supported Au–Pd core-shell nanoparticles within a dihexadecylphosphate film for the development of hydrazine electrochemical sensor, *Sensors and Actuators B* **256** (2018) 535-542. https://doi.org/10.1016/j.snb.2017.10.107

[9] J. Liu, J. Jiang, Y. Dou, F. Zhang, X. Liu, J. Qu, Q. Zhu, A novel chemiluminescent probe for hydrazine detection in water and HeLa cells, *Organic & Biomolecular Chemistry* **17(29)** (2019) 6975-6979. https://doi.org/10.1039/C9OB01407A

[10] J.-A. Oh, J.-H. Park, H.-S. Shin, Sensitive determination of hydrazine in water by gaschromatography–mass spectrometry after derivatization with ortho phthalaldehyde, *Analytica Chimica Acta* **769** (2013) 79-83. https://doi.org/10.1016/j.aca.2013.01.036

[11] Z. Wang, Y. Zhang, Z. Meng, M. Li, C. Zhang, L. Yang, Y. Yang, X. Xu, S. Wang, Development of a ratiometric fluorescent probe with large Stokes shift and emission wavelength shift for real-time tracking of hydrazine and its multiple applications in environmental analysis and biological imaging, *Journal of Hazardous Materials* **422** (2022) 126891. https://doi.org/10.1016/j.jhazmat.2021.126891

[12] S. Ayaz, Y. Dilgin, R. Apak, Flow injection amperometric determination of hydrazine at a cupric-neocuproine complex/anionic surfactant modified disposable electrode, *Microchemical Journal* **159** (2020) 105457. https://doi.org/10.1016/j.microc.2020.105457

[13] A. S. Amosov, N. V. Ul'yanovskii, D. S. Kosyakov, O. A. Shpigun, Simultaneous determination of hydrazine, methylhydrazine, and 1,1-dimethylhydrazine by high-performance liquid chromatography with pre-and post-column derivatization by 5-nitro-2-furaldehyde, *Journal of Analytical Chemistry* **73** (2018) 497-503. https://doi.org/10.1134/S1061934818050027

[14] B. Zargar, A. Hatamie, A simple and fast colorimetric method for detection of hydrazine in water samples based on formation of gold nanoparticles as a colorimetric probe, *Sensors and Actuators B* **182** (2013) 706-710. https://doi.org/10.1016/j.snb.2013.03.036

[15] A. Mahieddine, L. Adnane-Amara, Constructing and electrochemical performance of NiCo-LDHs@ h-Ni NWs core–shell for hydrazine detection in environmental samples. *Journal of Electroanalytical Chemistry* **930** (2023) 117168. https://doi.org/10.1016/j.jelechem.2023.117168

[16] M. Alsaiari, A. R.Younus, A. Rahim, R. Alsaiari, N. Muhammad, An electrochemical sensing platform of cobalt oxide@SiO_2/C mesoporous composite for the selective determination of

hydrazine in environmental samples, *Microchemical Journal* **165** (2021) 106171. https://doi.org/10.1016/j.microc.2021.106171

[17] Z. Meng, B. Liu, M. Li, A sensitive hydrazine electrochemical sensor based on Ag-Ni alloy/reduced graphene oxide composite, *International Journal of Electrochemical Science* **12(11)** (2017) 10269-10278. https://doi.org/10.20964/2017.11.15

[18] N. S. K. Gowthaman, B. Sinduja, S. A. John, Tuning the composition of gold–silver bimetallic nanoparticles for the electrochemical reduction of hydrogen peroxide and nitrobenzene, *RSC Advances* **6(68)** (2016) 63433-63444. https://doi.org/10.1039/C6RA05658J

[19] D. Mohapatra, N. S. K. Gowthaman, M. S. Sayed, J.-J. Shim, Simultaneous ultrasensitive determination of dihydroxybenzene isomers using GC electrodes modified with nitrogen-doped carbon nano-onions, *Sensors and Actuators B* **304** (2020) 127325. https://doi.org/10.1016/j.snb.2019.127325

[20] N. S. K. Gowthaman, M. A. Raj, S. A. John, Nitrogen-doped graphene as a robust scaffold for the homogeneous deposition of copper nanostructures: A nonenzymatic disposable glucose sensor, *ACS Sustainable Chemistry & Engineering* **5(2)** (2017) 1648-1658. https://doi.org/10.1021/acssuschemeng.6b02390

[21] M. M. I. Khan, M. A. Yousuf, P. Ahamed, M. Alauddin, N. T. Tonu, Electrochemical Detection of Dihydroxybenzene Isomers at a Pencil Graphite Based Electrode, *ACS Omega* **7(33)** (2022) 29391-29405. https://doi.org/10.1021/acsomega.2c03651

[22] Y. Shao, Y. Zhu, R. Zheng, P. Wang, Z. Zhao, J. An, Highly sensitive and selective surface molecularly imprinted polymer electrochemical sensor prepared by Au and MXene modified glassy carbon electrode for efficient detection of tetrabromobisphenol A in water, *Advanced Composites and Hybrid Materials* **5(4)** (2022) 3104-3116. https://doi.org/10.1007/s42114-022-00562-8

[23] B. J. Ostertag, M. T. Cryan, J. M. Serrano, G. Liu, A.E. Ross, Porous carbon nanofiber-modified carbon fiber microelectrodes for dopamine detection, *ACS Applied Nano Materials* **5(2)** (2022) 2241-2249. https://doi.org/10.1021/acsanm.1c03933

[24] J. Zoubir, N. Bougdour, W. El Hayaoui, C. Radaa, A. Idlahcen, A. Assabbane, I. Bakas, Electrochemical detection of metronidazole using silver nanoparticle-modified carbon paste electrode, *Electrocatalysis* **13(4)** (2022) 386-401. https://doi.org/10.1007/s12678-022-00722-w

[25] A. Kasaeinasab, H. A. Mahabadi, S. J. Shahtaheri, F. Faridbod, M. R. Ganjali, F. Mesgari, Carbendazim trace analysis in different samples by using nanostructured modified carbon paste electrode as voltametric sensor, *PLoS One* **18(1)** (2023) e0279816. https://doi.org/10.1371/journal.pone.0279816

[26] P.-S. Ganesh, A.B.Teradale, S.-Y. Kim, H.-U. Ko, E.E. Ebenso, Electrochemical sensing of anti-inflammatory drug mesalazine in pharmaceutical samples at polymerized-congo red modified carbon paste electrode, *Chemical Physics Letters* **806** (2022) 140043. https://doi.org/10.1016/j.cplett.2022.140043

[27] Z. Deng, Z. Wu, M. Alizadeh, H. Zhang, Y. Chen, C. Karaman, Electrochemical monitoring of 4-chlorophenol as a water pollutant via carbon paste electrode amplified with Fe_3O_4 incorporated cellulose nanofibers (CNF), *Environmental Research* **219** (2023) 114995. https://doi.org/10.1016/j.envres.2022.114995

[28] T. S. S. Kumar Naik, B. E. Kumara Swamy, S. Singh, J. Singh, E. I. Naik, G. K. Jayaprakash, P. C. Ramamurthy, Fabrication and theoretical analysis of sodium alpha-olefin sulfonate-anchored carbon paste electrode for the simultaneous detection of adrenaline and paracetamol, *Journal of Applied Electrochemistry* **52(41)** (2022) 697-708. https://doi.org/10.1007/s10800-021-01663-w

[29] M. Yu, L. Wu, J. Miao, W. Wei, A. Liu, S. Liu, Titanium dioxide and polypyrrole molecularly imprinted polymer nanocomposites based electrochemical sensor for highly selective

detection of p-nonylphenol, *Analytica Chimica Acta* **1080** (2019) 84-94. https://doi.org/10.1016/j.aca.2019.06.053

[30] J. Ai, X. Wang, Y. Zhang, H. Hu, H. Zhou, Y. Duan, D. Wang, H. Wang, H. Du, Y. Yang, A sensitive electrochemical sensor for nitenpyram detection based on CeO_2/MWCNTs nanocomposite, *Applied Physics A* **128(9)** (2022) 831. https://doi.org/10.1007/s00339-022-05952-9

[31] N. F. Atta, A. Galal, A. R. M. El-Gohary, Gold-doped nano-perovskite-decorated carbon nanotubes for electrochemical sensing of hazardous hydrazine with application in wastewater sample, *Sensors and Actuators B* **327** (2021) 128879. https://doi.org/10.1016/j.snb.2020.128879

[32] B. Patella, C. Sunseri, R. Inguanta, Nanostructured based electrochemical sensors, *Journal of Nanoscience and Nanotechnology* **19(6)** (2019) 3459-3470. https://doi.org/10.1166/jnn.2019.16110

[33] M. Imran, S. Ahmed, A. Z. Abdullah, J. Hakami, A. A. Chaudhary, H. A. Rudayni, S.-U.-D. Khan, A. Khan, N. S. Basher, Nanostructured material-based optical and electrochemical detection of amoxicillin antibiotic, *Luminescence* **38(7)** (2023) 1064-1086. https://doi.org/10.1002/bio.4408

[34] R. Ali, M. M. El-Wekil, Construction of MIP/Bi_2S_3 nanoparticles/rGO nanoprobe for simultaneous electrochemical determination of amoxicillin and clavulanic acid, *Journal of Alloys and Compounds* **962** (2023) 171180. https://doi.org/10.1016/j.jallcom.2023.171180

[35] N. S. K. Gowthaman, D. Mohapatra, P. Arul, W. S. Chang, Ultrasonic-assisted decoration of AuNPs on carbon nano-onions as robust electrochemical scaffold for sensing of carcinogenic hydrazine in industrial effluents, *Journal of Industrial and Engineering Chemistry* **117** (2023) 227-237. https://doi.org/10.1016/j.jiec.2022.10.009

[36] N. S. K. Gowthaman, H. N. Lim, V. Balakumar, S. Shankar, Ultrasonic synthesis of CeO_2@organic dye nanohybrid: environmentally benign rabid electrochemical sensing platform for carcinogenic pollutant in water samples, *Ultrasonics Sonochemistry* **61** (2020) 104828. https://doi.org/10.1016/j.ultsonch.2019.104828

[37] E. Narayanamoorthi, P. Arul, N. S. K. Gowthaman, S. A. John, Morphology dependent electrocatalytic activity of copper based porous organic frameworks via diverse chain length of linkers and counterions of metal precursor, *Electrochimica Acta* **409** (2022) 139994. https://doi.org/10.1016/j.electacta.2022.139994

[38] W. Choi, N. Choudhary, G. H. Han, J. Park, D. Akinwande, Y. H. Lee, Recent development of two-dimensional transition metal dichalcogenides and their applications, *Materials Today* **20(3)** (2017) 116-130. https://doi.org/10.1016/j.mattod.2016.10.002

[39] S. Velmurugan, S. Palanisamy, T. C.-K. Yang, Single-crystalline SnS_2 nano-hexagons based non-enzymatic electrochemical sensor for detection of carcinogenic nitrite in food samples, *Sensors and Actuators B* **316** (2020) 128106. https://doi.org/10.1016/j.snb.2020.128106

[40] B. D. Bhat, Tuning the magnetic and electronic properties of monolayer SnS_2 by 3d transition metal doping: A DFT study, *Materials Today Communications* **33** (2022) 104626. https://doi.org/10.1016/j.mtcomm.2022.104626

[41] Q. Sun, D. Li, L. Dai, Z. Liang, L. Ci, Structural engineering of SnS_2 encapsulated in carbon nanoboxes for high-performance sodium/potassium-ion batteries anodes, *Small* **16(45)** (2020) 2005023. https://doi.org/10.1002/smll.202005023

[42] D. Wang, X. Yan, C. Zhou, J. Wang, X. Yuan, H. Jiang, Y. Zhu, X. Cheng, R. Li, A free-standing electrode based on 2D SnS_2 nanoplates@3D carbon foam for high performance supercapacitors, *International Journal of Energy Research* **44(11)** (2020) 8542-8554. https://doi.org/10.1002/er.5540

[43] P. Bharathi, P. S. Harish, M. Shimomura, M. K. Mohan, J. Archana, M. Navaneethan, Controlled growth and fabrication of edge enriched SnS_2 nanostructures for room

temperature NO_2 gas sensor applications, *Materials Letters* **335** (2023) 133691. https://doi.org/10.1016/j.matlet.2022.133691

[44] L. Wang, Y. Wang, A. Zhang, Z. Wu, Fabrication of Ag/SnS_2/g-C_3N_4 Z-scheme-type hetero-junction photocatalysts with enhanced LED light-driven photoactivity, *Inorganic Chemistry Communications* **156** (2023) 111144. https://doi.org/10.1016/j.inoche.2023.111144

[45] R. Shanmugam, J. Ganesamurthi, T.-W. Chen, S.-M. Chen, K. Alagumalai, J. Alkahtani, M. S. Alwahibi, M. H. Ajmal Ali, Synergetic combination of nano hexagons SnS_2/Sulfur substituted graphitic carbon nitride: Evaluation of electrochemical sensor for the agricultural pollutant in environmental samples, *Chemical Engineering Journal* **431(Part 2)** (2022) 134174. https://doi.org/10.1016/j.cej.2021.134174

[46] R. Shanmugam, S. Manavalan, S.-M. Chen, M. Keerthi, L.-H. Lin, Methyl parathion detection using SnS_2/N, S–Co-doped reduced graphene oxide nanocomposite, *ACS Sustainable Chemistry & Engineering* **8(30)** (2020) 11194-11203. https://doi.org/10.1021/acssuschemeng.0c02528

[47] B. Yang, H. Li, C. Nong, X. Li, S. Feng, A novel electrochemical immunosensor based on SnS_2/NiCo metal-organic frameworks loaded with gold nanoparticles for cortisol detection, *Analytical Biochemistry* **669** (2023) 115117. https://doi.org/10.1016/j.ab.2023.115117

[48] M. Zhou, Y. Pu, Q. Wu, P. Wang, T. Liu, M. Zhang, 2D hexagonal SnS_2 nanoplates as novel co-reaction accelerator for construction of ultrasensitive g-C_3N_4-based electrochemiluminescent biosensor, *Sensors and Actuators B: Chemical* **319** (2020) 128298. https://doi.org/10.1016/j.snb.2020.128298

[49] R. Rama, S. Meenakshi, K. Pandian, S. C. B. Gopinath, Room temperature ionic liquids-based electrochemical sensors: an overview on paracetamol detection, *Critical Reviews in Analytical Chemistry* **52(6)** (2022) 1422-1431. https://doi.org/10.1080/10408347.2021.1882834

[50] T. A. Silva, A. Wong, O. Fatibello-Filho, Electrochemical sensor based on ionic liquid and carbon black for voltammetric determination of Allura red colorant at nanomolar levels in soft drink powders, *Talanta* **209** (2020) 120588. https://doi.org/10.1016/j.talanta.2019.120588

[51] S. Šekuljica, V. Guzsvány, J. Anojčić, T. Hegedűs, M. Mikov, K. Kalcher, Imidazolium-based ionic liquids as modifiers of carbon paste electrodes for trace-level voltammetric determination of dopamine in pharmaceutical preparations, *Journal of Molecular Liquids* **306** (2020) 112900. https://doi.org/10.1016/j.molliq.2020.112900

[52] N. Alahmadi, H. S. Alhasan, H. Gomaa, A. A. Abdelwahab, M. Y. Emran, Electrochemical sensor design based on CuO nanosheets/Cellulose derivative nanocomposite for hydrazine monitoring in environmental samples, *Microchemical Journal* **183** (2022) 107909. https://doi.org/10.1016/j.microc.2022.107909

[53] Y. Dong, Z. Yang, Q. Sheng, J. Zheng, Solvothermal synthesis of Ag@Fe_3O_4 nanosphere and its application as hydrazine sensor, *Colloids and Surfaces A* **538** (2018) 371-377. https://doi.org/10.1016/j.colsurfa.2017.11.024